Simple method for improving the sampling in profile measurements by use of the Ronchi test

Josep Arasa, Santiago Royo, and Núria Tomàs

We present a simple method for increasing the number of data points obtained during performance of profilometric measurements with the Ronchi test. The method is based on multiple ronchigram acquisitions that are superimposed after a few very simple data-processing operations. The measurement method, experimental setup, and data processing are described in detail from the ronchigram to the measured profile, and experimental results for a concave surface of an spherical ophthalmic lens are provided. The radius of curvature values measured for that surface are compared with the ones obtained with a high-precision radioscope, showing very good agreement and demonstrating the capability of the technique to measure topographic profiles of reflective samples. © 2000 Optical Society of America

OCIS codes: 120.3930, 120.3940, 120.4800, 120.6650, 120.4290.

1. Introduction

The Ronchi test has long been used as a measuring tool in the optical shop.[1] The technique allows the measurement of highly aberrated wave fronts, owing to its ability to measure large ray slope changes, but lacks the sampling and accuracy properties now commonplace in other optical profilometry techniques. It has been described with the same mathematical theory as the well-known Hartmann screen test,[2] and also as a shearing interferometer.[3] Considerable research has been developed on accuracy improvements of Ronchi-test techniques through phase-shifting schemes.[4,5]

However, solutions aimed at improving the number of measured data points on the surface being tested are not so usual. In this paper we present an improvement of the Ronchi-test technique that is easy to set up and allows a significant increase in the number of data points measured. The principle of measurement and the experimental arrangement is described, including the experimental setup and the data-processing procedures being used to extract a surface profile from the registered fringe patterns. Next, the presented technique is applied to profile an spherical sample, and the accuracy of the measurement is validated by comparison of a reference radius of curvature with the radius of curvature obtained by surface fitting an spherical surface to the measured profile. Finally, conclusions are drawn from the presented results.

2. Principle of Measurement

In Ronchi-test techniques the wave front being tested is sampled through a low-frequency grating consisting of light and dark stripes of equal pitch (the Ronchi ruling). The fringe pattern generated when the wave front being tested crosses the Ronchi ruling is then used to compute a reconstruction of the incoming wave front.

Figure 1 presents the Ronchi-test experimental setup we used. An optical fiber forms an almost point-shaped diverging source (4 μm wide) that provides a diverging wave front. After reflection on a pellicle beam splitter, this wave front impinges on the reflective concave surface being tested. The reflected wave front, containing the information from the surface under test, passes through the beam splitter again, crosses a Ronchi ruling and the fringe pattern so created (which will be called the ronchigram henceforth) is recorded with a CCD camera with its objective focused on infinity.

Information on the position at the Ronchi ruling plane at which the rays reflected on the sample crossed the ruling may be obtained with the known

J. Arasa (arasa@oo.upc.es), S. Royo (royo@oo.upc.es), and N. Tomàs (tomas@oo.upc.es) are with the Center for the Development of Sensors, Instrumentation and Systems (CD6), Universitat Politècnica de Catalunya, Violinista Vellosolà 37 E-08222 Terrassa, Spain.

Received 3 January 2000; revised manuscript received 5 June 2000.

0003-6935/00/254529-06$15.00/0

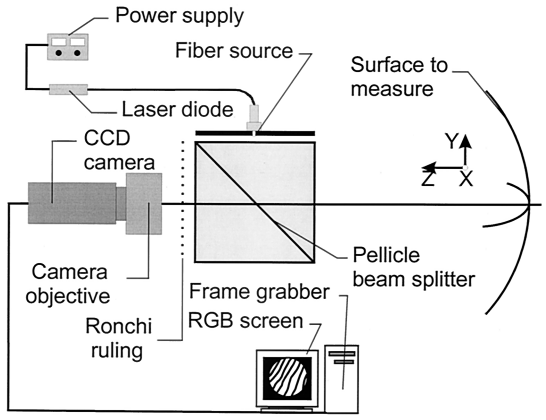

Fig. 1. Experimental setup.

period of the ruling and from one reference line whose absolute position is known. This allows the determination of the absolute position at the Ronchi ruling plane of each of the bright strips in the registered ronchigram. By use of the known focal length of the objective and the pixel pitch of the CCD array, the slope of the rays passing through each bright strip may be determined from the particular pixel on the CCD array on which the rays are impinging; this determination is possible because the camera objective has been focused on infinity and, under this working condition, all rays with a given slope impinge on a certain pixel (Fig. 2). Therefore, with one single ronchigram, the slope and position of a set of rays along the coordinate orthogonal to the ruling lines may be measured.

To obtain combined position and slope information of the wave front in two orthogonal directions, one can use two approaches. Either rotational symmetry of the wave front is assumed,[6] or a second ronchigram is obtained with the ruling lines tilted 90°.[7,8] We prefer this last approach, as a particular shape of the measured wave front is not assumed, yielding a more general measurement method. In our measurements, the ruling lines are placed horizontally in one ronchigram (following the X axis in Fig. 1) and vertically in the other (following the Y axis in Fig. 1). We refer to these ronchigrams as the X and the Y ronchigrams.

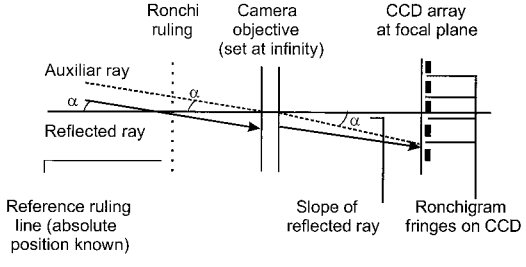

Fig. 2. Measurement of the slope and position of one ray reflected on the sample at the Ronchi ruling plane. With the objective focused at infinity, each pixel receives only rays with a given slope. Position at the ruling plane is obtained with a reference ruling line.

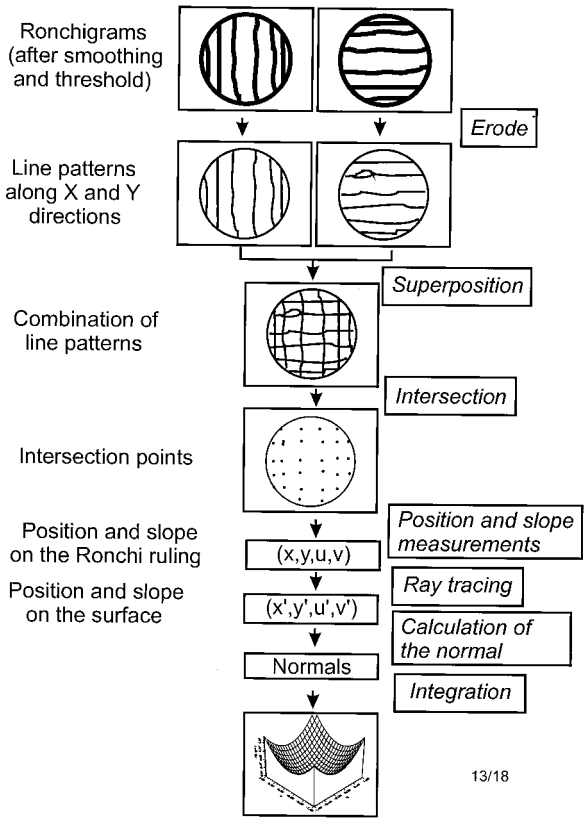

Fig. 3. Data processing from the ronchigram to the surface profile.

A set of usual image-processing operations are then performed, and a schematic data-processing sequence is provided in Fig. 3. The initial set of operations involves smoothing, thresholding, and eroding the bright strips on each ronchigram to obtain the one-pixel-wide central line in each bright strip. The eroded fringe patterns coming from the two orthogonal ronchigrams are then superimposed, and the intersection points of the line patterns from the X and the Y ronchigrams may be determined. At these intersection points the slope and incidence position along the X and the Y axes of a set of reflected rays is known at the Ronchi ruling plane.

By use of ray-tracing techniques (Fig. 4), the intersection of each reflected ray with the sample surface may then be obtained, provided that the source is

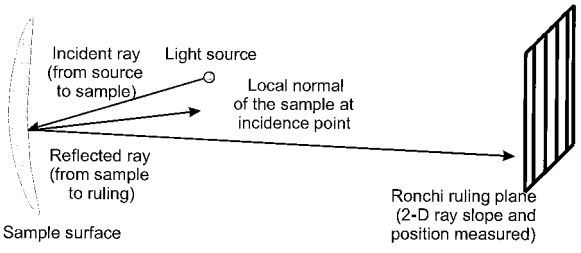

Fig. 4. Ray-tracing schematics. Reflected rays are ray traced backwards to calculate the local normal to the sample at the point where the rays leave the surface.

placed close to the center of curvature of the surface under test. This paraxial condition assumption greatly simplifies the ray-tracing procedures, as it allows for consideration of ray tracing from the Ronchi ruling plane to the tangent plane to the surface at its vertex as equivalent to ray tracing to the real surface.[9] The incident ray on the sample surface may be calculated as the one going from the source to the position on the sample surface where each reflected ray leaves the surface under test. Once the incident and reflected ray at a set of points of the surface are known, the local normal to the surface at those points is computed by use of Snell's law. A final integration procedure yields the desired surface profile, assuming the measured wave front is smooth. With this profile measurement technique, the number of measured data points on the surface is determined by the number of bright strips present in the acquired ronchigrams: the higher the number of bright strips, the higher the number of intersection points between them that become valid sampling points on the surface under test. Typical values involve approximately ten bright strips in each direction, yielding a typical value of 100 sampling points.

An apparent solution for improving the sampling of the surface under test would be to raise the frequency of the ruling to yield more strips in each recorded ronchigram. However, this approach would also increase the importance of the diffractive effects caused by the ruling in the ronchigram, up to a point at which the simple geometric description of the ronchigram used would not be valid. Frequencies of 70lpi ($T = 0.356$ mm) have been estimated as the maximum for the geometric approach to remain valid both theoretically and experimentally.[9]

The desired increase in the number of sampling points should increase the number of bright strips in the X and the Y ronchigrams without any undesired increase in the diffractive effects caused by the ruling. This is obtained if a number n of ronchigrams with the lines of the ruling displaced a fraction T/n of its period are recorded along the X and the Y axes, yielding n X ronchigrams and n Y ronchigrams. Each of these displaced ronchigrams then undergoes the same smoothing, thresholding, and eroding procedure previously mentioned, to be finally superimposed to yield a composed ronchigram. If each original ronchigram had m lines, the composed X ronchigram would have an estimate of $m \times n$ lines, and the same would apply for the Y ronchigram. The number of measured sampling points would rise from m^2 with one X ronchigram and one Y ronchigram to an estimated value of $(m \times n)^2$ with the described multiacquisition procedure. This means an increase of 2 orders of magnitude in the number of sampled points if $n = 10$, meaning that the lines of the ruling are displaced $T/10$ between consecutive ronchigram acquisitions.

To perform this multiacquisition procedure, it was necessary to include two encoder motors in the experimental setup; this allowed precise micrometric displacements of the Ronchi ruling along the X and the Y axes. It is stressed that, as the Ronchi ruling consists of straight light and dark stripes, displacement along the X(Y) axis keeps the X(Y) ronchigram unaltered. As typical displacement values need submicrometric accuracy, we named the technique microstepping. An additional stepping motor allowed rotation of the ruling around the Z axis to direct the lines on the ruling in the desired direction, with a resolution of 1.1×10^{-3} rad.

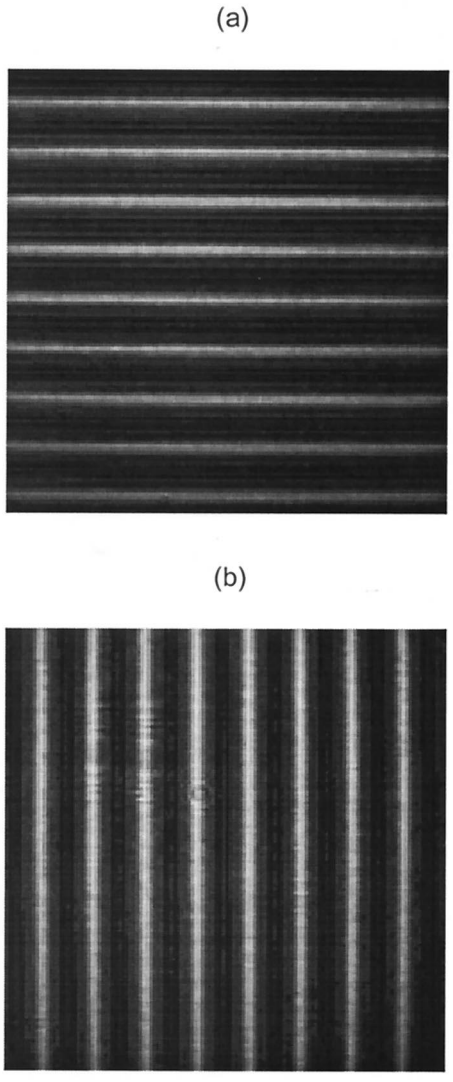

Fig. 5. First pair of ronchigrams: (a) ruling lines along the X axis (X ronchigram) and (b) ruling lines along the Y axis (Y ronchigram).

3. Experiment

Experimental results are presented for one spherical surface, which was measured with a high-precision radioscope to provide a reference value, yielding a radius of curvature of 149.7 mm. Comparison of this reference value with the radius of curvature value measured with the presented Ronchi-test technique is done to test the reliability of the measurement. Results are presented and compared for both the non-

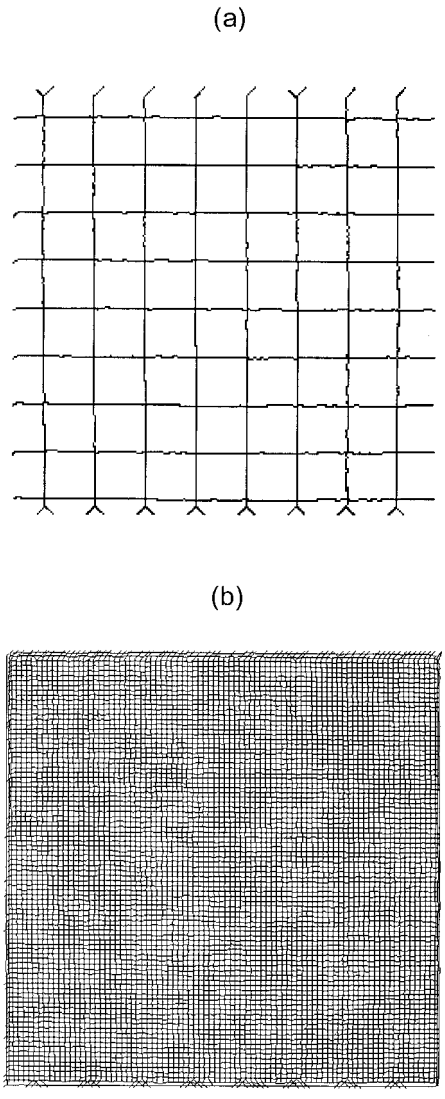

Fig. 6. Superposition of eroded ronchigrams. Each intersection of orthogonal lines is a valid sampling point. (a) Nonmicrostepped experiment and (b) microstepped experiment.

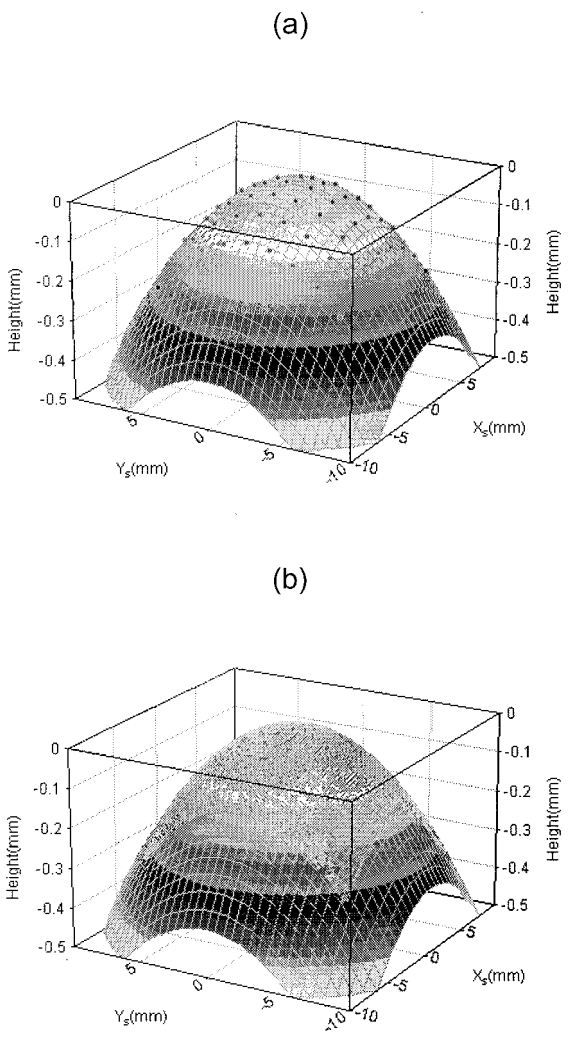

Fig. 7. Three-dimensional surface reconstruction: (a) nonmicrostepped experiment and (b) microstepped experiment.

microstepped and the microstepped experiment. A Ronchi ruling of 50 lines/in (T = 0.508 mm) was used, together with a fixed focal objective with 50-mm effective focal length at the CCD camera. The distance from the Ronchi ruling to the surface was set at 171.2 mm. Ten steps were performed in the microstepped experiment, so consecutive ronchigram data acquisitions were obtained when the ruling was displaced 50.8 μm.

Figure 5 shows the pair of ronchigrams obtained for the nonmicrostepped experiment, which are used as the first pair in the series of ten pairs of ronchigrams required in the microstepped experiment. Figure 6 shows the superposition of eroded ronchigrams in the nonmicrostepped and the microstepped experiments. The number of valid sampling points has risen from 72 to 7583 in the microstepped experiment, yielding the intensive sampling of the measured area observed in Fig. 6(b). The measured area in the microstepped and in the nonmicrostepped measurements are 2.04 and 1.76 cm^2, respectively.

When the data processing is completed, a surface profile is obtained in which a height value is assigned to each sampling point. Height values between sampling points are interpolated by use of any three-dimensional representation software used. With the larger number of sampled points available with microstepping techniques, the effect of these interpolation procedures is significantly reduced, as consecutive data points become much closer to each other. This effect may be observed in Fig. 7, in which the three-dimensional profile reconstruction for the surface being tested is presented both for the nonmicrostepped and the microstepped experiment. The plotted surface has been interpolated by software, and the available data points have been plotted on it as dots. Figure 8 presents the same data again under a contour plot representation, without any software interpolation, meaning that each of the plotted points is a measured data point from the surface, with a gray value determined by its measured height.

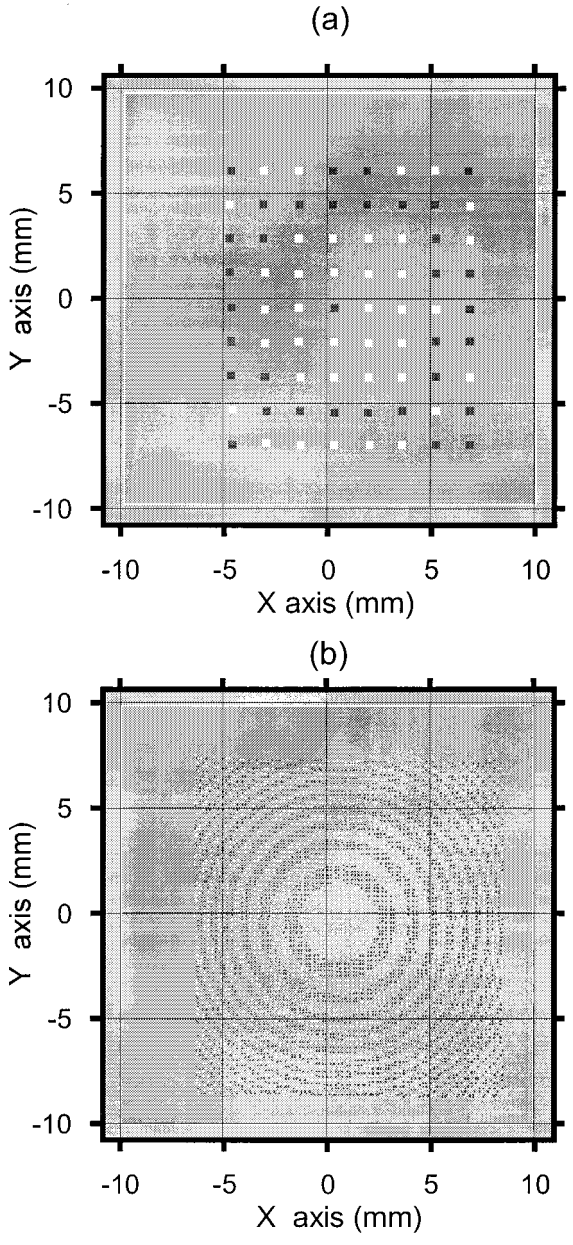

Fig. 8. Contour plot surface reconstruction: (a) nonmicrostepped experiment, contour step 72 μm and (b) microstepped experiment, contour step 9 μm. Data points in the nonmicrostepped experiment have been enlarged to improve their visibility. Each plotted point is a measured data point with a gray value determined by its measured height.

Each contour step equals 72 μm in Fig. 8(a) and 9 μm in Fig. 8(b). Even with the higher contour step values, the spherical shape of the surface is hardly appreciated in Fig. 8(a), in which points with available data have been enlarged to a 5×5 pixel square to improve its visibility. In Fig. 8(b), the amount of plotted points in the microstepped experiment allows a much more detailed picture of the measured surface, and the effect of the improvement of the sampling in the quality of the measurement may be appreciated.

Table 1. Three-Dimensional Fitting Results for the Measured Surface with Eq. (1)[a]

Measurement Procedure	R (mm)	x_0 (mm)	y_0 (mm)	r^2
Nonmicrostepped	149.78	0.66	0.03	0.999998
Microstepped	149.78	0.66	0.03	0.999998

[a] R is the radius of curvature of the best-fit sphere; (x_0, y_0) are the coordinates of the vertex of the surface; and r^2 is the correlation coefficient of the fit.

To test the validity of the measurement procedure, we fit the microstepped and nonmicrostepped sets of measured (x, y, z) data to the best spherical surface, described by

$$z = \frac{\frac{1}{R}\left[(x - x_0)^2 + (y - y_0)^2\right]^{1/2}}{1 + \left[1 - \frac{(x - x_0)^2 + (y - y_0)^2}{R^2}\right]^{1/2}}, \qquad (1)$$

where z is the sagitta of the surface, R is its radius of curvature, and $(x_0, y_0, 0)$ are the coordinates of its vertex. The radius of curvature and vertex position values yielding the spherical surface that best fits the measured (x, y, z) values are shown in Table 1, together with the correlation coefficient depicting the quality of the fit.

It may be seen how the measured radius of curvature values of both microstepped and nonmicrostepped measurements agree very well with the 149.7-mm value used as reference. The closeness of the correlation coefficient to unity also demonstrates the similarity of the measured surface to the spherical shape described in Eq. (1). It is worth noting that the values obtained in both measurements are identical up to the 0.01-mm scale in radius of curvature and in vertex position, confirming that the microstepped and the nonmicrostepped measurements are obtaining the same surface profile, although with a different number of sampling points. This provides consistent proof of the capability of the technique to measure topographic profiles of concave surfaces.

Even though the profiles in Figs. 8(a) and 8(b) are quite different visually, the results of the curve-fitting procedure have not been noticeably affected by the microstepping procedure. Although the number of measured data points is reduced in the nonmicrostepped measurement, they all belong to the same sphere, so its fitting yields identical results. As a consequence, the microstepping method is not required during measurement performed just to obtain radius of curvature values, although they provide a very important improvement in the sampling of the topographic measurements performed with Ronchi-test techniques.

4. Conclusions

In summary, a simple experimental technique to improve the sampling in Ronchi-test techniques has

been presented. The technique is based on multiple ronchigram acquisition through small motorized displacements of the Ronchi ruling in two orthogonal directions. Data from the acquired ronchigrams is superimposed to obtain more sampling points on the surface without increasing the diffractive effects caused by the Ronchi ruling.

The technique increases the sampling of the measurement by a factor n^2 when n ronchigrams in orthogonal directions are recorded, providing a simple way to perform intensive samplings of the surfaces being tested and to minimize the effects of software interpolation in neighboring data points when the profile of the surface is plotted. Results have been presented for a concave spherical sample and validated with radioscopic radius of curvature measurements, showing the accuracy of the measurement technique.

References

1. A. Cornejo-Rodríguez, "Ronchi test," in *Optical Shop Testing*, 2nd ed., D. Malacara, ed. (Wiley, New York, 1992), Chap. 9.
2. A. Cordero-Dávila, A. Cornejo-Rodríguez, and O. Cardona-Núñez, "Ronchi and Hartmann tests with the same mathematical theory," Appl. Opt. **31,** 2370–2376 (1992).
3. K. Patorski, "Heuristic explanation of grating shearing interferometry using incoherent illumination," Opt. Acta **31,** 33–38 (1984).
4. T. Yatagai, "Fringe scanning Ronchi test for aspherical surfaces," Appl. Opt. **23,** 3676–3679 (1984).
5. K. Hibino, D. I. Farrant, B. K. Ward, and B. F. Oreb, "Dynamic range of Ronchi test with a phase-shifted sinusoidal grating," Appl. Opt. **36,** 6178–6189 (1997).
6. A. Cornejo and D. Malacara, "Ronchi test of aspherical surfaces, analysis, and accuracy," Appl. Opt. **9,** 1897–1901 (1970).
7. M. P. Rimmer and J. C. Wyant, "Evaluation of large aberrations using a lateral-shear interferometer having variable shear," Appl. Opt. **14,** 142–150 (1975).
8. W. Meyers and H. P. Stahl, "Contouring of a free oil surface," in *Interferometry, Techniques and Analysis*, G. M. Brown, O. Y. Kwon, M. Kujawinska, and G. T. Reid, eds. Proc. SPIE **1755,** 84–94 (1992).
9. S. Royo, "Topographic measurements of non-rotationally symmetrical surfaces using Ronchi deflectometry," Ph.D. dissertation (Technical University of Catalonia, Terrassa, Spain, 1999).